



# HHS Public Access

Author manuscript

*Cancer Gene Ther.* Author manuscript; available in PMC 2010 October 01.

Published in final edited form as:

*Cancer Gene Ther.* 2010 April ; 17(4): 244–255. doi:10.1038/cgt.2009.70.

## Enhanced Specific Delivery and Targeting of Oncolytic Sindbis Viral Vectors by Modulating Vascular Leakiness in Tumor

Jen-Chieh Tseng, PhD, Tomer Granot, BS, Vincent DiGiacomo, MS, Brandi Levin, BS, and Daniel Meruelo, PhD

NYU Cancer Institute and the NYU Gene Therapy Center, Department of Pathology, NYU School of Medicine, New York University, 550 First Avenue, New York, NY 10016

### Summary

Genetic instability of cancer cells generates resistance after initial responses to chemotherapeutic agents. Several oncolytic viruses have been designed to exploit specific signatures of cancer cells, such as important surface markers or pivotal signaling pathways for selective replication. It is less likely for cancer cells to develop resistance given that mutations in these cancer signatures would negatively impact tumor growth and survival. However, as oncolytic viral vectors are large particles, they suffer from inefficient extravasation from tumor blood vessels. For larger particles, such as viral vectors, their ability to reach cancer cells is an important consideration in achieving specific oncolytic targeting and potential vector replication. Our previous studies indicated that the Sindbis viral vectors target tumor cells via the laminin receptor (LAMR). Here, we present evidence that modulating tumor vascular leakiness, using VEGF and/or metronomic chemotherapy regimens significantly enhances tumor vascular permeability and directly enhances oncolytic Sindbis vector targeting in tumor models. Since host-derived vascular endothelium cells are genetically stable and less likely to develop resistance to chemotherapeutics, a combined metronomic chemotherapeutics and oncolytic viruses regimen should provide a new approach for cancer therapy. This mechanism could explain the synergistic treatment outcomes observed in clinical trials of combined therapies.

### Keywords

Sindbis virus; viral vector; cancer; vascular leakiness; molecular imaging; chemotherapy

### Introduction

The goal of cancer gene therapy is to achieve specific and efficient delivery of gene therapy vectors to tumor cells while reducing the impact of unwanted toxicity, associated with the vector of choice, to normal tissues. In addition, to maximize therapeutic effects, an ideal vector system should be able to achieve systemic delivery, via the bloodstream, to distal or metastasized tumor cells. Several viral vector systems have been developed to specifically

Users may view, print, copy, download and text and data- mine the content in such documents, for the purposes of academic research, subject always to the full Conditions of use: [http://www.nature.com/authors/editorial\\_policies/license.html#terms](http://www.nature.com/authors/editorial_policies/license.html#terms)

Correspondence to: D. Meruelo, dm01@mac.com, telephone number: (212) 263-5599, fax: (212) 263-8211.

transduce tumor cells by modification of viral structural proteins 1–4, or to selectively replicate in tumors by taking advantage of tumor specific signaling pathways 5, 6. Currently, however, only a few viral vector systems, among which is Sindbis vector 7, are capable of systemic delivery without dramatically reducing efficacy. Along with tumor specificity and systemic delivery, a vector must efficiently penetrate tumor vascular structures in order to reach and transduce cancer cells.

Tumor growth depends upon angiogenesis and many cancer therapy agents have been developed to target newly formed tumor blood vessels 8. Unlike normal vessels, the endothelium cells in tumor vessels are less organized and unusually leaky 9. Abnormal blood vessel leakiness has been known in tumors, and higher levels of leakiness correlate with histological grade and malignancy 10. The vessel leakiness can cause extravasations of plasma proteins and even erythrocytes in some extreme cases (hemorrhage). These phenomena have been supported by evidence from several experimental tumors, including extravasations of small soluble tracers such as radioisotopes, albumin, dextran, as well as larger particles such as colloidal carbon and liposomes up to 2  $\mu\text{m}$  in size 11–13. Intratumoral hemorrhage is an extensive form of vascular leakiness, which ranges from scattered extravasated erythrocytes to a blood lake, consisting of larger collections of erythrocytes surrounded by tumor cells 14, 15. Such vessel leakiness may be the direct result of hyperactive angiogenesis and vascular remodeling in tumors. On the other hand, increased leakiness of tumor vessels allows deeper penetration and may provide a means to selectively deliver cancer therapeutic agents into tumor tissues. In particular, tumor vessel leakiness should play an important role in the delivery of larger therapeutic agents, such as oncolytic viruses, into tumors.

Our previous findings indicate that vectors based on the Sindbis virus are capable of systemic tumor targeting via the bloodstream 7. Immunohistochemistry data indicate that the vector targets tumor tissue closely associated with vascular structure 16. Sindbis vector targets laminin receptor (LAMR) on cancer cells for specific binding and infection 17. Intracellular LAMR precursor (37-Kda LRP) is crucial for cellular ribosomal function 18, while its mature 67-Kda form is important to mediate cancer cell migration and metastasis 19. Furthermore, LAMR seems to be essential for cell survival. The importance of LAMR for oncogenesis makes Sindbis vector suitable for oncolytic purposes. Also, the fact that Sindbis transduction causes tumor death by inducing apoptosis 20–22, even without adding cytotoxic payload genes, makes Sindbis derived vectors promising therapeutic agents for cancer therapy 16, 23, 24.

In this report we used an oncolytic vector system based on Sindbis virus to achieve selective targeting and replication in tumors. Two types of vector systems have been adopted for use of cancer gene therapy. The replication-defective (RD) vector system is capable of transient transgene expression by replacing the viral structural gene with desired therapeutic gene 25. Taking advantage of the viral subgenomic promoter, the RD system is capable of high-level transgene expression. We previously demonstrated the use of RD Sindbis viral vector to detect and monitor tumors in small laboratory animals using molecular imaging methods, such as bioluminescence 7 and positron emission tomography (PET) 26. The second type of Sindbis vector is replication competent (RC). Another set of subgenomic promoter is

harnessed to drive the expression of viral structure genes 27. Thus the RC Sindbis vector has great oncolytic potential to infect, proliferate and spread within the tumor.

Several chemotherapy agents have been developed for first-line treatments of cancer, including taxanes (paclitaxel and docetaxel) and platinum-based drugs (cisplatin, carboplatin, and oxaliplatin). These drugs do not specifically target tumor cells, but rather interfere with cell division. For example, paclitaxel blocks microtubule disassembly during mitosis. Cisplatin causes DNA damage resulting in cell-cycle checkpoint and apoptosis. Therefore, in addition to cancer cells, these drugs also damage normal dividing cells of tissues with rapid regeneration, such as bone marrow, hair follicles and gut mucosa. As a result, most chemotherapeutic agents have narrow therapeutic indexes due to high host toxicity.

Cancer cells are not the only rapidly dividing cells in tumors. Dividing endothelial cells in growing blood vessels in tumors should also be susceptible to chemotherapeutic agents 28. Furthermore, as endothelial cells originate from normal host tissues, they are assumed to be more genetically stable and carry less genetic defects than cancer cells. This feature makes endothelial cells less likely than cancer cells to develop drug resistance especially after prolonged treatments of chemotherapy. Therefore, cancer cells that are resistant to a particular chemotherapy agent could indirectly respond to the agent through an attack of the tumor vasculature. Damaged tumor blood vessels may result in increased vascular permeability.

Little is known about the correlation between vector delivery/transduction kinetics and tumor vascular leakiness. In this report, we provide *in vivo* bio-optical imaging evidence that specific transduction of Sindbis vector directly correlates with vascular leakiness in tumors. Furthermore, enhancing tumor vessel leakiness using a vector carrying a vascular endothelium growth factor gene (VEGF) or co-treatment using chemotherapy agents, such as paclitaxel and cisplatin, greatly enhances vector delivery and transduction in tumors. Our results suggest that, in addition to strategies currently used involving tumor specific surface markers or cancer-type specific signaling features, modulation of tumor vascular leakiness could provide an additional layer of tumor specificity. Thus, the capability to manipulate tumor vessel leakiness could be an important tool to achieve improved cancer gene therapy using oncolytic viruses, especially due to their intrinsically larger size compared with other smaller agents.

## Materials and Methods

### Cells and vector preparation

Hamster BHK and mouse N2a cells (American Type Culture Collection, Manassas, VA) are maintained in  $\alpha$ MEM (JRH Bioscience, Lenexa, KS) with 5% FBS and in Eagle-modified media (MEM, JRH Bioscience) with 10% FBS, respectively. ES-2/Fluc cells were derived from human ES-2 ovarian cancer cells 29, and were maintained in McCoy's 5A medium (Mediatech, Inc., Herndon, VA) with 10% FBS.

Constructions of RD-Sindbis/Fluc and/LacZ are previously described 7. RD-Sindbis/mPlum was constructed by insertion of a DNA fragment encoding the mPlum protein (from pmPlum plasmid, Clontech Laboratories Inc., Mountain View, CA) into pSinRep5 replicon plasmid at the *PmlI* site. We performed similar procedures to generate RD-Sindbis/VEGF using a DNA fragment from pBLAST49-mVEGF plasmid (InvivoGen Inc., San Diego, CA). Production of Sindbis vector particles are achieved by *in vitro* transcription of replicon (from pSinRep5) and helper (from pDH-BB) RNAs, followed by electroporation of both replicon and helper RNAs into BHK cells as previous described 16. A replication-competent (RC) Sindbis/Fluc vector was constructed by insertion of a second subgenomic promoter and viral structural genes downstream of firefly luciferase gene as previously described 27.

## Imaging

Qtracker® 800 quantum dot was obtained from Molecular Probes Inc. (Eugene, OR). AngioSense® 750 was purchased from VisEn Medical (Bedford, MA). The fluorescent imaging was done using IVIS® Spectrum imaging system (Caliper Life Sciences, Inc., Hopkinton, MA). Each image of indicated excitation/emission matrix was acquired for 1 sec at aperture setting of f4. The raw sequential imaging data were analyzed using the Living Image® 3.0 software (Caliper Life Science, Inc.) to unmix concentration maps for Qtracker and AngioSense.

All animal experiments were performed in accordance with NIH and institutional guidelines. BHK cells ( $1.5 \times 10^6$ /mouse) were s.c. inoculated into SCID mice (female, 6–8 week old, Taconic, Germantown, NY). The mouse neuroblastoma tumors were induced by s.c. injection of  $1.5 \times 10^6$  N2a cells into SCID mice 13 days prior to treatments. For better visualization, we remove excessive fur on the skin over the tumor and its surrounding region. The setting for dual mPlum/AngioSense imaging is as following: ex605/em660, 680 and 700 nm, followed by ex745/em800, 820 and 840 nm. Bioluminescent imaging of luciferase activities was performed as described before 7. Tumor sizes were measured using the formula:  $\pi/6 \times \text{length (mm)} \times \text{width (mm)}^2$ .

## Statistical analysis

We used Prism® 4 for Macintosh (GraphPad Software, Inc., La Jolla, CA) to perform statistical analysis of our data. Quantitative imaging data and tumor growth curves were analyzed using Two-way ANOVA or *t*-test. Survival data were analyzed using Kaplan-Meier log-rank test. All *P* values generated were in two-tailed.

## Results

### Near-infrared (NIR) fluorescent imaging of tumor vessel leakiness *in vivo*

In order to visualize tumor vessels and vascular leakiness, we used two different near-infrared (NIR) fluorescent probes, Qtracker and AngioSense, for *in vivo* molecular imaging of tumor vasculature. Qtracker is a non-targeted fluorescent nanoparticle (20–50 nm in diameter) with a broad excitation wavelength (400–700 nm) and an emission wavelength at around 800 nm. The surfaces of these quantum dots are chemically modified to reduce non-specific binding and immune responses, making Qtracker a useful imaging tool for *in vivo*

imaging of tumor vessels with minimal leakage from the vasculature. The rigid sphere shape of the nanoparticle makes Qtracker stable in circulation. In contrast, AngioSense is a smaller and flexible NIR fluorescent macromolecule (250k MW). Unlike Qtracker, AngioSense has a narrower excitation wavelength at 750 nm and an emission wavelength at around 800 nm. AngioSense is designed as a NIR imaging probe for vascularity, perfusion and vascular permeability. Although both NIR probes have similar emission wavelength at ~800 nm, it is possible to distinguish their specific distribution by using different excitation wavelengths (~500 nm for Qtracker and ~750 nm for AngioSense).

Taking advantage of our IVIS spectrum imaging system, which is capable of acquiring sequential fluorescent excitation-emission images of the same subject, we intravenously injected the Qtracker/AngioSense mixture into a tumor-bearing mouse to determine if we could visualize general tumor vessel structure and vascular leakiness (Figure 1). A severe combined immunodeficiency (SCID) mouse, bearing a subcutaneous (s.c.) BHK tumor, was used for its known vascular leakiness for Sindbis vector delivery. To visualize general vascular structure, we performed the first sequential imaging matrix 100 min after tracer administration via the tail vein (Figure 1a). For leakiness imaging, a second imaging matrix was performed 24 hour after tracer injection (Figure 1a). The reconstructed concentration maps at 100 min indicate that both Qtracker and AngioSense signals have similar distribution patterns that identify general vessels in the tumor (Figure 1b, green arrows). However, the 24 hr concentration maps suggest that the Qtracker signals still retain a similar distribution pattern as before, while the AngioSense develops a more disperse and widespread pattern than the 100 min images, indicating vascular leakiness in these regions (Figure 1b, red arrows). In addition, the IVIS spectrum system is capable of analyzing the excitation-emission matrix and generates a reconstructed concentration map of Qtracker and AngioSense in each mouse (Figure 1c). These data indicate that while AngioSense is capable of imaging general vascular structure within a short period time (<3 hrs) after its administration, prolonged incubation ( 24 hrs) provides a means to visualize leaky tumor vasculature.

### **Sindbis viral vector transduction correlates with tumor vessel leakiness**

Having established the ability to visualize leaky vascular regions in tumors, we tested if there is a correlation between tumor leakiness and Sindbis vector transduction. In the first set of experiments we used a replication-defective vector carrying the *mPlum* gene. Originally derived from DsRed protein, mPlum fluorescent protein has a red-shifted functional spectrum (ex: 590 nm; em: 650 nm) suitable for *in vivo* imaging.

On day 0, a single dose of intravenous (i.v.) RD-Sindbis/mPlum vector was injected into a SCID mouse bearing a s.c. BHK tumor. A single dose of AngioSense was also i.v. administrated on the same day and the first IVIS imaging matrix for both mPlum and Angiosense signals was acquired 2 hrs after AngioSense injection (Figure 2a, Day 0). Follow-up images of mPlum expression and AngioSense retention in the tumor were acquired on day 1, 2, 3, 4, and 7. For simplicity, Figure 2a only shows the images of the optimal excitation-emission pairs for mPlum (ex605/em660 nm) and AngioSense (ex745/em800 nm). AngioSense signal on day 0 only shows the major tumor vessels since the

majority of the tracer is still in free circulation. Starting on day 1, as circulating AngioSense starts to extravasate from leaky blood vessels and is retained in surrounding tumor tissues, we were able to distinguish tumor regions that showed higher vascular permeability. This process requires a period of time (>24 hrs) in order to achieve sufficient contrast for imaging tumor vascular leakiness. After a single injection, the tumor AngioSense signals are retained for about 24–48 hours and gradually fade away starting at 72 hours.

A bio-fluorescent marker, such as mPlum, requires a higher level of expression for IVIS detection. That none or very little of mPlum signal was detected in the tumor during the first 24 hrs (Figure 2a, Day 0 and 1) was not surprising, since the vector needs some time to amplify sufficient mPlum protein for IVIS detection. Starting on day 2, tumor-specific mPlum signals were observed in tumor regions whose size and shape are very similar to day 1 AngioSense signals (green arrow), suggesting that the initial RD-Sindbis/mPlum transduction occurred at the viable tumor regions that have high vascular leakiness. Also, the AngioSense signal pattern on day 2 indicated that the tumor was expanding and there was a region showing exclusion of the probe (gray arrow). Sindbis infection is known to cause apoptosis and tumor necrosis 16, 20–22. The loss of AngioSense signals indicated necrotic tumor tissue with reduced permeability. By day 3, when the mPlum signal became very strong, most of the mPlum positive regions seemed to correlate with the necrotic tumor region. Due to probe excretion from the urinary track (as evident by strong bladder signal on day 2), the AngioSense signals started to fade away on day 3 and very little remained by day 7. On the other hand, mPlum signals remained in necrotic tumor tissue and were detectable until day 7, suggesting that sufficient mPlum protein, which was produced inside tumor cells after Sindbis/mPlum transduction, remained within the necrotic tissue thereafter.

To verify that the necrotic tumor region was caused by Sindbis/mPlum transduction, we reconstructed the concentration maps of mPlum and AngioSense using the imaging data set obtained on day 3 (Figure 2b). The necrotic tumor tissue is not autofluorescent under the mPlum imaging setting due to its more red shift properties. As shown in the composite image, the fact that both mPlum and AngioSense signals are distinctively present strongly suggests that the necrotic region is directly caused by Sindbis transduction. This result is in accordance with our previous histology data that indicates Sindbis-induced apoptosis and tumor necrosis occurs within 2–3 days 16.

We believe that the vector is able to transduce tumor and express transgene during the first 24 hrs. The fact that we were not able to detect mPlum expression during the first 24 hrs is likely due to technical limitation of the bio-fluorescent protein, which is intrinsically less sensitive and requires a higher level for *in vivo* imaging compared with bio-luminescent luciferase methods. Unlike the RD-Sindbis/mPlum vector that requires more than 1 day to visualize tumor-specific transduction, a parallel experiment using the RD-Sindbis/Fluc vector indicates that firefly luciferase provided better sensitivity. We were able to detect tumor-specific luciferase signal on day 1 (Figure 2c). In addition, the luciferase signals correlated nicely with the leaky vasculature as indicated by AngioSense signals. These results support our hypothesis that vascular leakiness is important for Sindbis vector tumor targeting.

### **VEGF enhances tumor vascular leakiness and promotes Sindbis vector transduction**

We tested whether enhancing tumor vascular leakiness would benefit Sindbis vector delivery and transduction in tumors. A replication-defective vector (RD-Sindbis/VEGF) was constructed to deliver a mouse vascular endothelial growth factor (VEGF) gene. Besides playing a key role in regulating blood vessel growth in both normal and pathological conditions, VEGF was first identified as a vascular permeability factor (VPF) 30. VEGF treatments on endothelial cells enable passage of particles of different sizes through vessels by a variety of physical mechanisms. In experimental tumors, the functional limits and defined pore cutoff sizes of transvascular transport induced by VEGF is believed to range from 200 nm to 1.2  $\mu\text{m}$  11–13. This level of vascular permeability would allow larger particles, such as Sindbis viral vectors (~70 nm in diameter), to extravasate into tumor tissues.

Since the RD-Sindbis/VEGF does not carry a reporter gene for imaging, we used a mixture of RD-Sindbis/VEGF and RD-Sindbis/Fluc vectors (1:1) to evaluate specific tumor transduction in the SCID/BHK s.c. tumor model. Utilizing a mixture of vectors does not necessarily mean co-expression of both VEGF and Fluc genes in the same cells. Rather, the enhanced vascular leakiness and vector delivery by VEGF would be reflected by increased Fluc signals within the tumor. A vector mixture of RD-Sindbis/LacZ:RD-Sindbis/Fluc (1:1) was used as a control. The animals received four daily intraperitoneal (i.p.) vector treatments from day 0–3. For imaging vascular leakiness in tumors, we only intravenously (i.v.) injected the AngioSense once on day 1. Intraperitoneal treatments of the RD VEGF/Fluc mixture significantly enhanced tumor vascular leakiness as evidenced by increased AngioSense signals (Figure 3a and b). As expected, higher vessel leakiness in RD VEGF/Fluc treated tumors resulted in higher RD-Sindbis/Fluc transduction (Figure 3c and d). As early as day 2 (Figure 3c), we observed significantly higher luciferase signals in tumors treated with RD VEGF/Fluc mixture, indicating that the vector is capable of transducing and expressing sufficient VEGF during the first 48 hrs of the treatments. In subsequent treatments, the vector system is capable of expressing sufficient VEGF during the first 24 hrs (Figure 2c). This result supports the idea of modulating tumor vessel leakiness in order to improve viral vector delivery and transduction.

### **Chemotherapeutic agents synergize with Sindbis vector in tumor eradication**

In order to test whether chemotherapeutic agents synergize with Sindbis vector in tumor eradication, we used our previously established ES-2/Fluc ovarian cancer model 29. I.p. inoculation of SCID mice with ES-2/Fluc cells results in widespread metastases in the peritoneal cavity. Tumor growth can be monitored using IVIS to detect the firefly luciferase activity of the cells (Figure 4a and b). A suitable chemotherapeutic agent is paclitaxel, since it has been shown to inhibit tumor angiogenesis at low concentration and endothelium cells are 10–100 times more sensitive to this agent than tumor cells 31–34. As expected, combined treatments of paclitaxel (at 16 mg/Kg on day 1, 4, 7 and 11) and RD-Sindbis/LacZ (daily from day 1–11) significantly reduce tumor burden and suppress tumor growth during the course of treatments (Figure 4a). Paclitaxel treatment alone only slows down the tumor growth but it is unable to reduce tumor load even after repeated treatments (Figure 4b). RD-Sindbis/LacZ alone showed better tumor killing during initial treatments compared with

Taxol. However, tumor load recovery on day 10 suggests that the vector only kills tumor cells it can reach during initial treatments, while unreachable tumor cells continue to grow.

The effectiveness of combined therapy is also reflected by the prolonged survival observed (Figure 4c). The combined therapy group (Taxol RD-LacZ) had the longest median survival, which is 36 days, compared with 17 days of the untreated control group, 28 days of the RD-LacZ treatment group, or 32 days of the Taxol treatment group ( $P < 0.0001$ ,  $n = 9$ , log-rank analysis of trend). By day 46, three mice survived in the combined therapy group while only one survived in the Taxol only group. IVIS imaging revealed that few of ES2Fluc tumor cells remained in the combined therapy group (Figure 4d). The results suggest that paclitaxel increases vessel permeability thereby enhancing the therapeutic effects of Sindbis vector. However, this result cannot rule out the possibility that paclitaxel simply kills more tumor cells without extensively damaging tumor blood vessels.

### **Chemotherapeutic agents and VEGF increase vessel leakiness and enhance therapeutic efficacy of oncolytic RC-Sindbis vectors**

In order to determine whether chemotherapeutic agents synergize with oncolytic RC-Sindbis vector in tumor eradication by modulating vascular leakiness, we used a s.c. mouse N2a neuroblastoma model. N2a neuroblastoma tumors are well vascularized and therefore are suitable to test any modulation of vascular leakiness that would enhance Sindbis vector transduction. However, Sindbis vector has a lower infectivity in N2a cells compared with BHK cells (about 1000 time less). To compensate, we used an oncolytic replication-competent (RC) Sindbis/Fluc vector 27 instead of an RD one to further enhance the tumor transduction signal output in N2a tumors. RC vector carries a full set of viral structural genes to support its replication. Specific tumor infection of RC vector could result in oncolytic effects by intratumoral vector replication and amplification. We also tested if the combination VEGF and paclitaxel further promote RC-Sindbis vector replication in tumors. Since prolonged expression of VEGF might promote tumor growth, we used replication defective RD-Sindbis/VEGF mixed with RC-Sindbis/Fluc (1:1) to ensure temporary expression of VEGF in tumor. Therefore, after the mixture vector treatments, a persistent tumor luciferase activity indicates successful delivery, infection, and propagation within tumors, or in other words, demonstrates successful oncolytic activity.

To test if chemotherapeutic agents enhance the propagation and spreading of oncolytic RC vector in tumors after initial infection, we only treated the mice with the vector mixtures (RD-VEGF/RC-Fluc or RD-LacZ/RC-Fluc) once at the beginning of treatments (day 0), following by repeated treatments of Taxol on day 1, 3 and 6. AngioSense was injected on day 1 and the retention kinetics in tumors was monitored on day 1, 2, 3 and 6 (Figure 5a and b). The VEGF gene alone significantly enhances AngioSense retention in tumors ( $P = 0.0476$ ), as well as to the same extent as does Taxol treatment ( $P = 0.0114$ ). The combination effects of VEGF and Taxol further increase the vascular leakiness in the N2a tumors ( $P = 0.0291$ ). In addition, the analysis of the AngioSense data on day 6 (Figure 5c), when most of the free circulating AngioSense tracer has been cleared from the body, shows significant retention in tumors treated with RD-VEGF alone ( $P = 0.022$ ), or with Taxol



alone ( $P = 0.0045$ ). The combined Taxol/RD-VEGF treatments further enhance the vascular leakiness ( $P = 0.035$ ).

The Taxol treatments enhance vascular leakiness that in turn supports active *in situ* replication and propagation of RC-Fluc in N2a tumors (Figure 5d and e). The luciferase signals observed in tumors are from active replication (or oncolytic) activity of RC-Fluc vectors. RD vectors (VEGF or LacZ) can only temporarily infect and express its transgenes. Without repeated Taxol treatments, the oncolytic activities of RC-Fluc was only short-lived, suggesting failure to actively propagate in the tumor. Temporal expression of VEGF by RD-VEGF can achieve a brief enhancement, but it gradually faded away by day 6 due to the apoptotic nature of the vector 16. However, in a combination of RD-VEGF and Taxol, the RC-Fluc can achieve better active oncolytic activities ( $P = 0.038$ ). The effectiveness of combined therapy is also reflected by diminished tumor growth (Figure 5f).

We also tested if another chemotherapy agent, cisplatin, has similar effects if metronomically administrated. As with Taxol, Cisplatin treatments significantly increased vascular permeability in s.c. N2a tumors (Figure 6a), and enhanced oncolytic transduction of RC-Sindbis/Fluc (Figure 6b). Better therapeutic efficacy was also observed in combined therapy (Figure 6c). These results support the idea that chemotherapeutic agents may improve the therapeutic outcome of oncolytic viral vectors by enhancing tumor vessel permeability and vector delivery.

## Discussion

In this report, we use novel molecular imaging techniques to visualize the correlation between tumor vascular leakiness and oncolytic vector delivery. Our results indicate that blood vessel permeability in tumors plays a significant role in successful vector targeting. Sindbis virus is considered a small virus with an average size of 60–70 nm in diameter, compared with other viruses recently developed for gene therapy purposes (adenovirus 90–100 nm, vesicular stomatitis virus 65–185 nm, and lentivirus 95–175 nm). Combined with its natural blood-borne capability, the smaller size makes Sindbis vectors suitable for systemic delivery. However, viral vectors are very large in comparison with chemotherapeutic agents. Methods to enhance vessel permeability may dramatically enhance the therapeutic efficacy of viral vectors against cancer. Using bio-optical NIR probes, we can specifically determine vascular leakiness and establish the kinetics of Sindbis vector transduction in tumors. This method should be of significant value for studying physiological conditions in tumors during or after oncolytic viral treatments.

VEGF was first identified as a vascular permeability factor (VPF) 30, and subsequent studies revealed the importance of VEGF in tumor vascular development and angiogenesis. However, the fact that VEGF-induced angiogenesis does not require VEGF-induced vascular permeability suggests that these two functions of VEGF are separate entities 35. In short-term, VEGF-mediated vascular permeability leads to accumulation of a fibrin barrier around tumors 36, which may limit their malignant properties. VEGF modulates endothelial cell-cell junctions, including adherens, tight and gap junctions, via signaling of Src family

kinases and/or various protein tyrosine phosphatases (PTP) 37. These short-term functions of VEGF increase permeability without the need of genomic replication of cellular DNA.

However, the negative impacts of prolonged expression of VEGF, by promoting vascular development in tumors, may outweigh the benefits of the VEGF-induced vascular leakiness. Although tumors naturally expressing high levels of VEGF may provide an additional layer of specificity for Sindbis targeting, it is known that long-term expression of VEGF would promote tumor angiogenesis and metastasis 38. Since elevated VEGF expression is associated with many human cancers 39, several oncolytic viral strategies have been designed to target neovasculature 40, 41 or to suppress VEGF activities in tumors. The combined anti-VEGF therapies, either using shRNA 42, soluble VEGF receptor 43, or co-treatment of anti-VEGF antibody 44, are aimed to inhibit the long-term functions of VEGF that promote new blood vessel formation and tumor growth. Such pro-angiogenic function of VEGF can be suppressed by metronomic agents, and thus counteract any residual pro-angiogenic property of the administered VEGF.

In normal tissue, prolonged expression of VEGF would cause inflammation 45, 46. Thus, to avoid the long-term expression, we propose the use of a RD vector system for VEGF gene delivery, which ensures temporary expression of VEGF at initial infection sites. Such limited expression could prevent tumor related angiogenesis, as a result of prolonged exposure of VEGF, while providing sufficient vessel permeability to maintain active oncolytic replication of RC Sindbis vectors within tumors (Figure 5). The increased vessel permeability would also promote subsequent distribution and spreading of the oncolytic vector from cell to cell within tumors after initial transduction.

By targeting rapidly dividing cells, conventional cytotoxic chemotherapy agents affect not only proliferating tumor cells but also various types of normal cells, such as those of the bone marrow, the hair follicles, the gut mucosa and, more importantly, the endothelium of the growing tumor vasculature 28. The anti-angiogenic effects of chemotherapy could indirectly contribute to their anti-tumor efficacy. By administering such drugs in small doses on a frequent schedule or “metronomically” (weekly, several times a week or daily), their anti-angiogenic effects seem to be enhanced and maintained for prolonged periods 28. In addition, this mechanism could explain the better and synergetic treatment outcomes observed in clinical trials of combined oncolytic viruses (such as Onyx-015) and chemotherapeutics 47.

Traditionally, conventional chemotherapy has been administered at more toxic “maximum tolerated dose” (MTD), which requires 2~3-week breaks between successive cycles of therapy for patients to recover from myelosuppression. However, such long periods of time may cause repair of tumor vasculature, since the proportion of dividing endothelial cells in tumor blood vessels might be too low for the MTD chemotherapy regimen to have significant impact 48. After cancer cells, due to their intrinsic genetic instability, acquire resistance to chemotherapy agents, MTD regimens could counteract the potential benefit of anti-angiogenic effects. By contrast, many studies of preclinical models indicate that metronomic chemotherapy is effective in treating tumors in which the cancer cells have developed resistance to the same chemotherapeutics 49. Thus, metronomic chemotherapy

regimens have the advantage of being less acutely toxic, making prolonged treatments and suppressing angiogenesis possible. For example, it has been shown that some metronomic regimens suppress circulating endothelial progenitor cells 48.

Combining metronomic chemotherapeutics with oncolytic vectors might be a promising strategy for cancer treatments. One immediate advantage is that chemotherapeutics induce damage in tumor blood vessels and increase vascular permeability for oncolytic vector delivery. Oncolytic viral vectors should retain efficacy in killing tumors that have developed resistance to conventional chemotherapeutic regimens. Since they are designed to selectively target cancer cells via tumor specific promoters or surface proteins that are important for cancer cell proliferation or survival, it is less likely that tumor cells will develop resistance to viral vectors. On the other hand, it is comparatively easier to acquire resistance to chemotherapeutics. One such example is the up-regulation of multidrug resistant 1 (*MDR1*) gene in human breast cancers, which encodes the P-glycoprotein drug-efflux pump 50. As a result, cancer cells can easily evade several chemotherapy drugs by modulating expression of a single gene. Therefore, combined metronomic-oncolytic vector regimens may provide new hope for cancer patients with relapsed disease due to acquired resistance after conventional MTD chemotherapy.

Of course, it is possible to envision a mechanism by which chemotherapeutics and/or VEGF directly enhance replication of the oncolytic vector in tumors instead of targeting tumor vasculature. However, this does not appear to be the case for paclitaxel, since pretreatment of cancer cells with the drug does not enhance vector replication and expression of reporter genes (data not shown). In addition, expression of VEGF doesn't increase the titer of Sindbis vector production.

Chemotherapeutics may have broad and complicated effects in tumors that contribute to the additive antitumor effects. In this study, our data indicate that one of the possible mechanisms is via modulation of vascular leakiness in tumors. In summary, the combined therapy takes advantage of the specific anti-tumor capability of oncolytic viral vectors and the modulation of angiogenesis by both viral vectors and chemotherapeutics.

## Acknowledgments

**Disclosure of support:** U.S. Public Health Service grants CA100687, and CA68498 from the National Cancer Institute, National Institutes of Health, and Department of Health and Human Services supported this study. Funding was also provided by a gift from the Litwin Foundation and a Research and License agreement between NYU and CynVec.

We thank Dr. Christine Pampero for critical reading of this manuscript and helpful discussions and we thank Mr. Seth Nickerson for constructing RD-Sindbis/mPlum vector. U.S. Public Health Service grants CA100687, and CA68498 from the National Cancer Institute, National Institutes of Health, and Department of Health and Human Services supported this study. Funding was also provided by a gift from the Litwin Foundation and a Research and License agreement between NYU and CynVec. The contents of this study are being utilized for a patent. According to the rules and regulations of New York University School of Medicine, if this patent is licensed by a third party, some of the authors (J. T., T. G., and D. M.) may receive benefits in the form of royalties or equity participation.

## References

1. Iijima Y, Ohno K, Ikeda H, Sawai K, Levin B, Meruelo D. Cell-specific targeting of a thymidine kinase/ganciclovir gene therapy system using a recombinant Sindbis virus vector. *Int J Cancer*. 1999; 80:110–8. [PubMed: 9935240]
2. Ohno K, Meruelo D. Retrovirus vectors displaying the IgG-binding domain of protein A. *Biochem Mol Med*. 1997; 62:123–7. [PubMed: 9367808]
3. Ohno K, Sawai K, Iijima Y, Levin B, Meruelo D. Cell-specific targeting of Sindbis virus vectors displaying IgG-binding domains of protein A. *Nat Biotechnol*. 1997; 15:763–7. [PubMed: 9255791]
4. Sawai K, Meruelo D. Cell-specific transfection of choriocarcinoma cells by using Sindbis virus hCG expressing chimeric vector. *Biochem Biophys Res Commun*. 1998; 248:315–23. [PubMed: 9675133]
5. Marcato P, Shmulevitz M, Lee PW. Connecting reovirus oncolysis and Ras signaling. *Cell Cycle*. 2005; 4:556–9. [PubMed: 15753655]
6. O'Shea CC. Viruses - seeking and destroying the tumor program. *Oncogene*. 2005; 24:7640–55. [PubMed: 16299526]
7. Tseng JC, Levin B, Hurtado A, Yee H, Perez de Castro I, Jimenez M, et al. Systemic tumor targeting and killing by Sindbis viral vectors. *Nat Biotechnol*. 2004; 22:70–7. [PubMed: 14647305]
8. Carmeliet P. Angiogenesis in life, disease and medicine. *Nature*. 2005; 438:932–6. [PubMed: 16355210]
9. Ribatti D, Nico B, Crivellato E, Vacca A. The structure of the vascular network of tumors. *Cancer Lett*. 2007; 248:18–23. [PubMed: 16879908]
10. McDonald DM, Baluk P. Significance of blood vessel leakiness in cancer. *Cancer Res*. 2002; 62:5381–5. [PubMed: 12235011]
11. Hobbs SK, Monsky WL, Yuan F, Roberts WG, Griffith L, Torchilin VP, et al. Regulation of transport pathways in tumor vessels: role of tumor type and microenvironment. *Proc Natl Acad Sci U S A*. 1998; 95:4607–12. [PubMed: 9539785]
12. Leunig M, Yuan F, Menger MD, Boucher Y, Goetz AE, Messmer K, et al. Angiogenesis, microvascular architecture, microhemodynamics, and interstitial fluid pressure during early growth of human adenocarcinoma LS174T in SCID mice. *Cancer Res*. 1992; 52:6553–60. [PubMed: 1384965]
13. Yuan F, Dellian M, Fukumura D, Leunig M, Berk DA, Torchilin VP, et al. Vascular permeability in a human tumor xenograft: molecular size dependence and cutoff size. *Cancer Res*. 1995; 55:3752–6. [PubMed: 7641188]
14. Liwnicz BH, Wu SZ, Tew JM Jr. The relationship between the capillary structure and hemorrhage in gliomas. *J Neurosurg*. 1987; 66:536–41. [PubMed: 3031239]
15. Van den Brenk HA, Crowe M, Kelly H, Stone MG. The significance of free blood in liquid and solid tumours. *Br J Exp Pathol*. 1977; 58:147–59. [PubMed: 861165]
16. Tseng JC, Levin B, Hirano T, Yee H, Pampeno C, Meruelo D. In vivo antitumor activity of Sindbis viral vectors. *J Natl Cancer Inst*. 2002; 94:1790–802. [PubMed: 12464651]
17. Wang KS, Kuhn RJ, Strauss EG, Ou S, Strauss JH. High-affinity laminin receptor is a receptor for Sindbis virus in mammalian cells. *J Virol*. 1992; 66:4992–5001. [PubMed: 1385835]
18. Ardini E, Pesole G, Tagliabue E, Magnifico A, Castronovo V, Sobel ME, et al. The 67-kDa laminin receptor originated from a ribosomal protein that acquired a dual function during evolution. *Mol Biol Evol*. 1998; 15:1017–25. [PubMed: 9718729]
19. Menard S, Tagliabue E, Colnaghi MI. The 67 kDa laminin receptor as a prognostic factor in human cancer. *Breast Cancer Res Treat*. 1998; 52:137–45. [PubMed: 10066078]
20. Griffin DE, Hardwick JM. Regulators of apoptosis on the road to persistent alphavirus infection. *Annu Rev Microbiol*. 1997; 51:565–92. [PubMed: 9343360]
21. Griffin DE, Hardwick JM. Perspective: virus infections and the death of neurons. *Trends Microbiol*. 1999; 7:155–60. [PubMed: 10217830]

22. Kerr DA, Larsen T, Cook SH, Fannjiang YR, Choi E, Griffin DE, et al. BCL-2 and BAX protect adult mice from lethal Sindbis virus infection but do not protect spinal cord motor neurons or prevent paralysis. *J Virol.* 2002; 76:10393–400. [PubMed: 12239316]
23. Venticinque L, Meruelo D. Sindbis viral vector induced apoptosis requires translational inhibition and signaling through Mcl-1 and Bak. 2008 Submitted.
24. Levine B, Huang Q, Isaacs JT, Reed JC, Griffin DE, Hardwick JM. Conversion of lytic to persistent alphavirus infection by the bcl-2 cellular oncogene. *Nature.* 1993; 361:739–42. [PubMed: 8441470]
25. Bredendiek PJ, Frolov I, Rice CM, Schlesinger S. Sindbis virus expression vectors: packaging of RNA replicons by using defective helper RNAs. *J Virol.* 1993; 67:6439–46. [PubMed: 8411346]
26. Tseng JC, Zanzonico PB, Levin B, Finn R, Larson SM, Meruelo D. Tumor-specific in vivo transfection with HSV-1 thymidine kinase gene using a Sindbis viral vector as a basis for prodrug ganciclovir activation and PET. *J Nucl Med.* 2006; 47:1136–43. [PubMed: 16818948]
27. Tseng JC, Daniels G, Meruelo D. Controlled propagation of replication-competent Sindbis viral vector using suicide gene strategy. *Gene Ther.* 2009; 16:291–6. [PubMed: 18818670]
28. Kerbel RS, Kamen BA. The anti-angiogenic basis of metronomic chemotherapy. *Nat Rev Cancer.* 2004; 4:423–36. [PubMed: 15170445]
29. Tseng JC, Hurtado A, Yee H, Levin B, Boivin C, Benet M, et al. Using sindbis viral vectors for specific detection and suppression of advanced ovarian cancer in animal models. *Cancer Res.* 2004; 64:6684–92. [PubMed: 15374985]
30. Senger DR, Galli SJ, Dvorak AM, Perruzzi CA, Harvey VS, Dvorak HF. Tumor cells secrete a vascular permeability factor that promotes accumulation of ascites fluid. *Science.* 1983; 219:983–5. [PubMed: 6823562]
31. Belotti D, Vergani V, Drudis T, Borsotti P, Pitelli MR, Viale G, et al. The microtubule-affecting drug paclitaxel has antiangiogenic activity. *Clin Cancer Res.* 1996; 2:1843–9. [PubMed: 9816139]
32. Grant DS, Williams TL, Zahaczewsky M, Dicker AP. Comparison of antiangiogenic activities using paclitaxel (taxol) and docetaxel (taxotere). *Int J Cancer.* 2003; 104:121–9. [PubMed: 12532428]
33. Ng SS, Figg WD, Sparreboom A. Taxane-mediated antiangiogenesis in vitro: influence of formulation vehicles and binding proteins. *Cancer Res.* 2004; 64:821–4. [PubMed: 14871806]
34. Pasquier E, Honore S, Pourroy B, Jordan MA, Lehmann M, Briand C, et al. Antiangiogenic concentrations of paclitaxel induce an increase in microtubule dynamics in endothelial cells but not in cancer cells. *Cancer Res.* 2005; 65:2433–40. [PubMed: 15781659]
35. Eliceiri BP, Paul R, Schwartzberg PL, Hood JD, Leng J, Cheresch DA. Selective requirement for Src kinases during VEGF-induced angiogenesis and vascular permeability. *Mol Cell.* 1999; 4:915–24. [PubMed: 10635317]
36. Brown LF, Dvorak AM, Dvorak HF. Leaky vessels, fibrin deposition, and fibrosis: a sequence of events common to solid tumors and to many other types of disease. *Am Rev Respir Dis.* 1989; 140:1104–7. [PubMed: 2478057]
37. Weis SM, Cheresch DA. Pathophysiological consequences of VEGF-induced vascular permeability. *Nature.* 2005; 437:497–504. [PubMed: 16177780]
38. Stacker SA, Caesar C, Baldwin ME, Thornton GE, Williams RA, Prevo R, et al. VEGF-D promotes the metastatic spread of tumor cells via the lymphatics. *Nat Med.* 2001; 7:186–91. [PubMed: 11175849]
39. Ferrara N. VEGF as a therapeutic target in cancer. *Oncology.* 2005; 69 (Suppl 3):11–6. [PubMed: 16301831]
40. Ong HT, Trejo TR, Pham LD, Oberg AL, Russell SJ, Peng KW. Intravascularly administered RGD-displaying measles viruses bind to and infect neovessel endothelial cells in vivo. *Mol Ther.* 2009; 17:1012–21. [PubMed: 19277014]
41. Liu TC, Castelo-Branco P, Rabkin SD, Martuza RL. Trichostatin A and oncolytic HSV combination therapy shows enhanced antitumoral and antiangiogenic effects. *Mol Ther.* 2008; 16:1041–7. [PubMed: 18388912]

42. Yoo JY, Kim JH, Kwon YG, Kim EC, Kim NK, Choi HJ, et al. VEGF-specific short hairpin RNA-expressing oncolytic adenovirus elicits potent inhibition of angiogenesis and tumor growth. *Mol Ther.* 2007; 15:295–302. [PubMed: 17235307]
43. Thorne SH, Tam BY, Kirn DH, Contag CH, Kuo CJ. Selective intratumoral amplification of an antiangiogenic vector by an oncolytic virus produces enhanced antivascular and anti-tumor efficacy. *Mol Ther.* 2006; 13:938–46. [PubMed: 16469543]
44. Libertini S, Iacuzzo I, Perruolo G, Scala S, Ierano C, Franco R, et al. Bevacizumab increases viral distribution in human anaplastic thyroid carcinoma xenografts and enhances the effects of E1A-defective adenovirus dl922-947. *Clin Cancer Res.* 2008; 14:6505–14. [PubMed: 18927290]
45. Mor F, Quintana FJ, Cohen IR. Angiogenesis-inflammation cross-talk: vascular endothelial growth factor is secreted by activated T cells and induces Th1 polarization. *J Immunol.* 2004; 172:4618–23. [PubMed: 15034080]
46. Lee CG, Link H, Baluk P, Homer RJ, Chapoval S, Bhandari V, et al. Vascular endothelial growth factor (VEGF) induces remodeling and enhances TH2-mediated sensitization and inflammation in the lung. *Nat Med.* 2004; 10:1095–103. [PubMed: 15378055]
47. Kumar S, Gao L, Yeagy B, Reid T. Virus combinations and chemotherapy for the treatment of human cancers. *Curr Opin Mol Ther.* 2008; 10:371–9. [PubMed: 18683102]
48. Bertolini F, Paul S, Mancuso P, Monestiroli S, Gobbi A, Shaked Y, et al. Maximum tolerable dose and low-dose metronomic chemotherapy have opposite effects on the mobilization and viability of circulating endothelial progenitor cells. *Cancer Res.* 2003; 63:4342–6. [PubMed: 12907602]
49. Browder T, Butterfield CE, Kraling BM, Shi B, Marshall B, O'Reilly MS, et al. Antiangiogenic scheduling of chemotherapy improves efficacy against experimental drug-resistant cancer. *Cancer Res.* 2000; 60:1878–86. [PubMed: 10766175]
50. Shen DW, Fojo A, Chin JE, Roninson IB, Richert N, Pastan I, et al. Human multidrug-resistant cell lines: increased *mdr1* expression can precede gene amplification. *Science.* 1986; 232:643–5. [PubMed: 3457471]

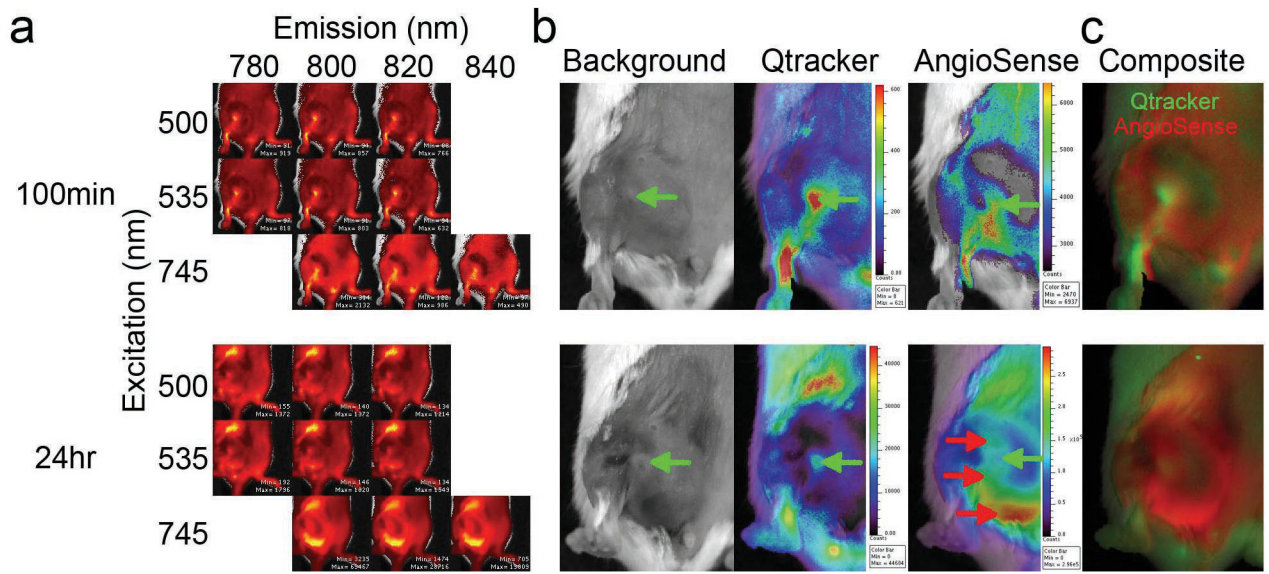


**Figure 1.**

Dual fluorescent imaging of tumor vasculature and its leakiness. In SCID mice carrying s.c. BHK tumors, both Qtracker and AngioSense detect tumor vasculature 100 min after i.v. injection of a 200  $\mu$ L mixture of both Qtracker (0.1  $\mu$ M) and AngioSense (3.3  $\mu$ M). However, the AngioSense can visualize tumor vascular leakiness after 24 hours of probe injection. (a) Raw image data after sequential acquiring of the indicated excitation/emission matrix. (b) The unmixed concentration maps for Qtracker and AngioSense. Green arrows indicate the initial tumor vasculature (Qtracker) and red arrows indicate subsequent regions with vessel leakiness. (c) The composite images of Qtracker (green) and AngioSense (red) signals.

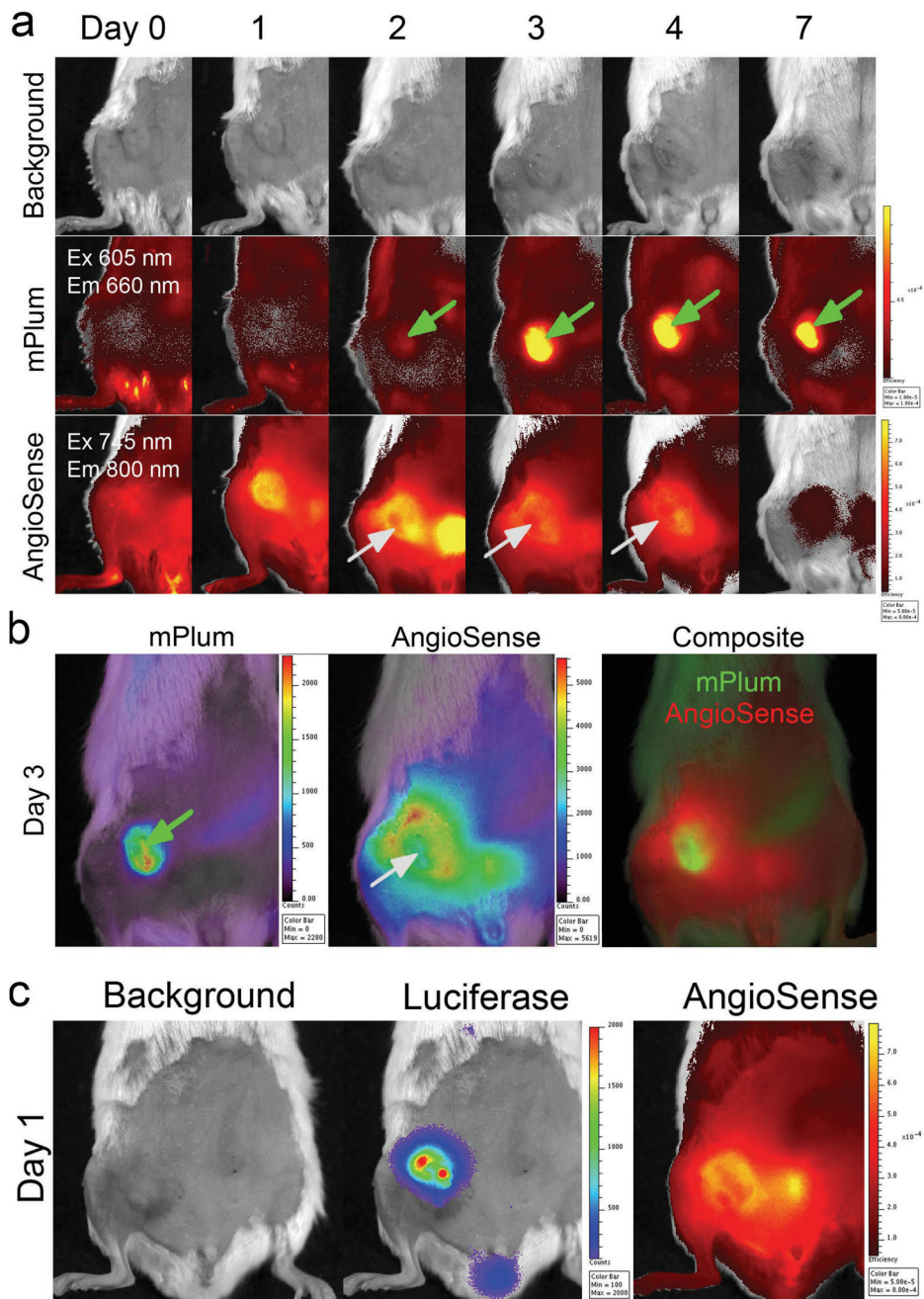


**Figure 2.** Sindbis viral vector transduces cancer cells via tumor vascular leakiness. **(a)** Kinetic images of SCID/BHK s.c. tumors after i.v. injection of AngioSense (0.66 nmol) and RD-Sindbis/mPlum ( $\sim 10^7$  particles) on day 0. Green arrows indicate positive mPlum fluorescent signals, and gray arrows indicate tumor necrosis resulted from Sindbis-induced apoptosis. **(b)** Reconstructed concentration maps for mPlum and AngioSense of the day 3 images. The mPlum signals are well associated with necrotic tumor tissue that shows little AngioSense signals. **(c)** Using a RD-Sindbis/Fluc vector that carries a firefly luciferase, instead of a



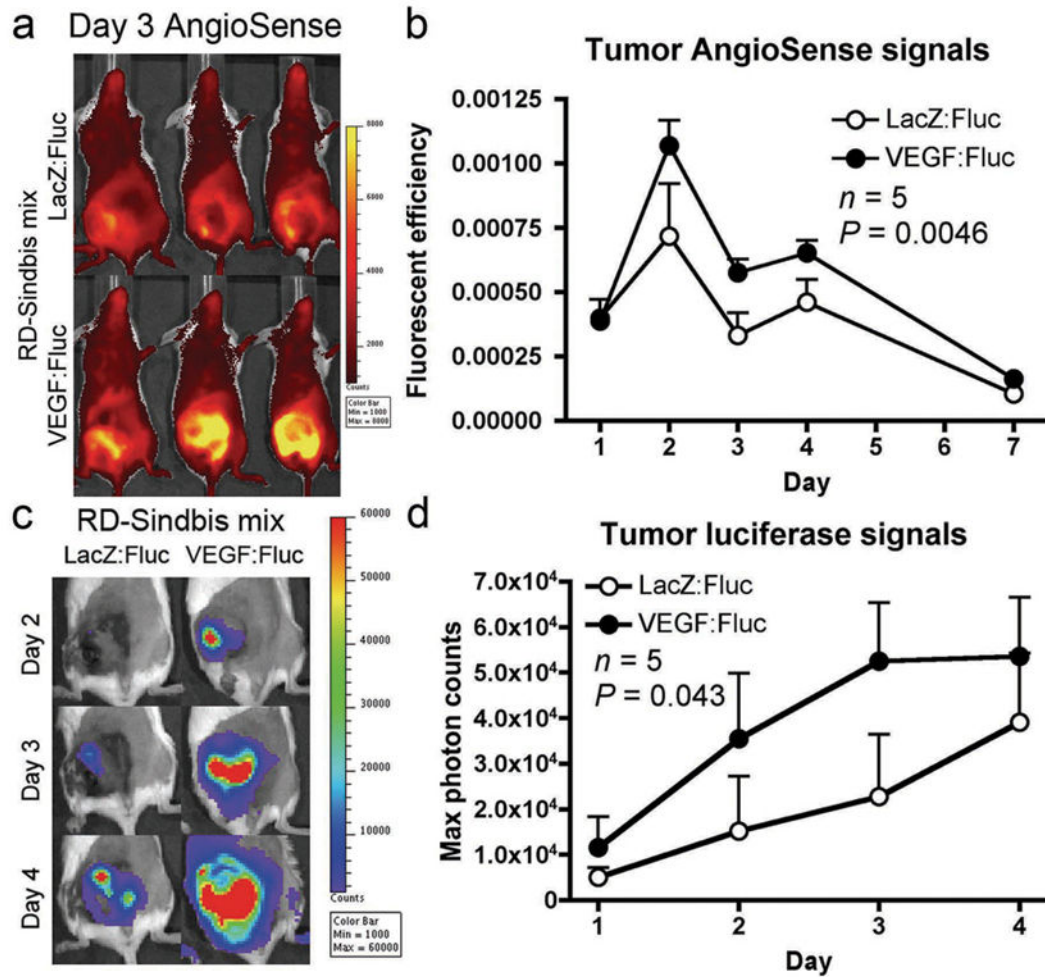
mPlum gene, enables detection of vector infection and its correlation with vascular leakiness as early as day 1.

Author Manuscript

Author Manuscript

Author Manuscript

Author Manuscript

**Figure 3.**

VEGF enhances tumor vascular leakiness and promotes Sindbis vector targeting. RD-Sindbis/VEGF vector ( $\sim 10^7$  particles/mL) were mixed with RD-Sindbis/Fluc vector ( $\sim 10^7$  particles/mL) at 1:1 ratio. A mixture of RD-Sindbis/LacZ and RD-Sindbis/Fluc was used as a control. SCID mice bearing s.c. BHK tumors received four daily i.p. treatments of vector mixture (500  $\mu$ L) from day 0–3. For imaging vascular leakiness in tumors, AngioSense 750 (0.66 nmol) was i.v. injected once on day 1. **(a)** AngioSense retention signal on day 3 shows enhancement of vascular permeability in the tumors of mice receiving the mixture containing RD-Sindbis/VEGF vectors. **(b)** AngioSense retention signals were analyzed in total fluorescent efficiency on day 1 (100 min after probe injection), 2, 3, 4 and 7. **(c)** Bioluminescent imaging of luciferase activities indicates VEGF promotes vector delivery and transduction. **(d)** Quantitative presentation of luciferase activities in tumors.

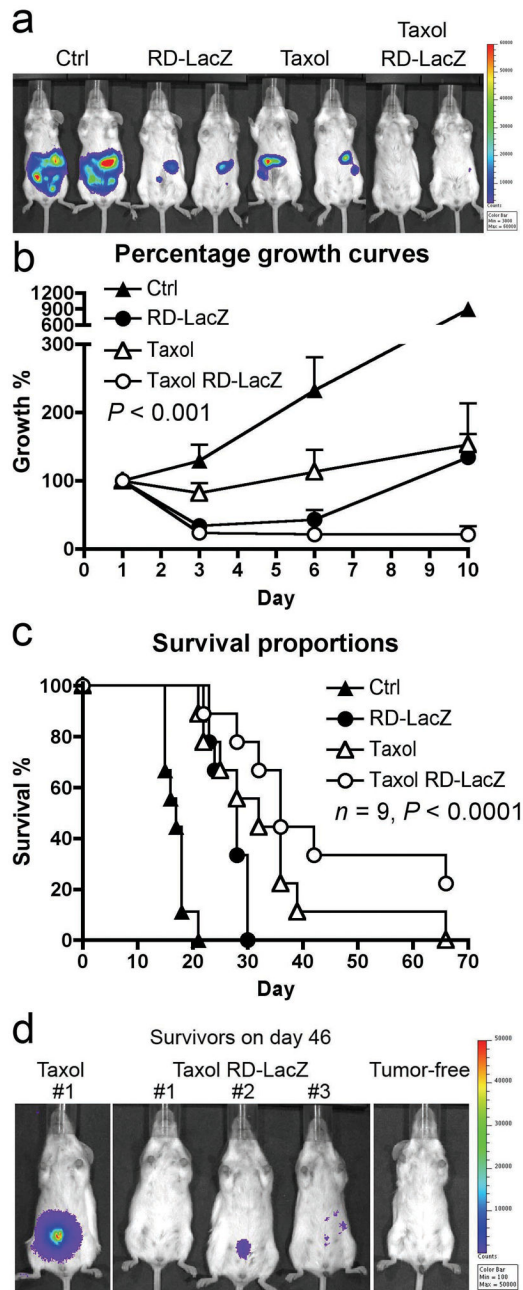


**Figure 4.**

Survival and tumor load in tumor-bearing mice treated with Sindbis and/or Taxol®. Mice were injected with  $4 \times 10^6$  ES2/Fluc cells on day 0. Mice were then divided into 4 groups of 9 animals, and were treated with Sindbis/LacZ (i.p.) daily from day 1 to day 11, and/or with Taxol® treatments (16 mg/Kg) on day 1, 4, 7 and 11. **(a)** Day 10 image. **(b)** Quantitative analysis of tumor growth, day 1 tumor load signal was set at 100% for each individual mouse for comparison with later images (day 3, 6, and 10). **(c)** Mouse survival was monitored and  $P$  value was generated by log-rank test of trend. **(d)** The surviving mice were imaged on day 46 to determine if they have any tumors.

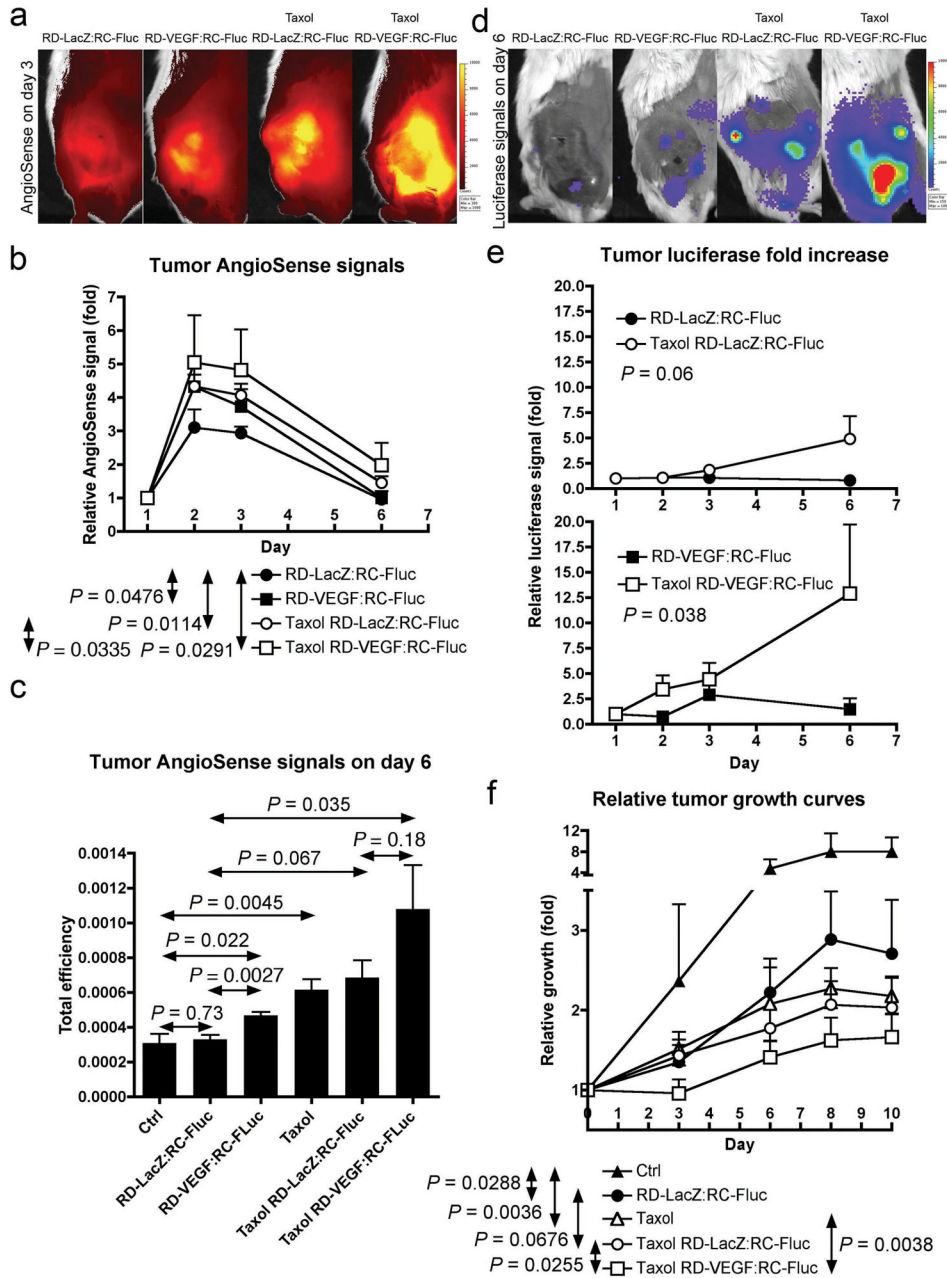


**Figure 5.** Paclitaxel enhances N2a tumor vascular leakiness and promotes propagation of oncolytic Sindbis vector after initial infection. On day 0, treatments of 1:1 mixture of RD-Sindbis/VEGF:RC-Sindbis/Fluc (0.5 mL, each has  $\sim 10^7$  particle/mL) were injected into tumor-bearing mice via the tail veins. We used 1:1 RD-Sindbis/LacZ:RC-Sindbis/Fluc mixture as a control. Persistent tumor luciferase activities indicate successful delivery, infection, and propagation within tumors. I.p. paclitaxel treatments (Taxol®, 16 mg/Kg or 48 mg/m<sup>2</sup> on day 1, 3 and 6, compared with maximum tolerated dose of 175 mg/m<sup>2</sup> in human) cause vascular insults and enhance tumor vascular leakiness. AngioSense 750 (0.66 nmol) was i.v. injected on day 1 and its retention kinetics was monitored on day 1, 2, 3 and 6. (a)

AngioSense imaging on day 3. **(b)** AngioSense retention kinetics and two-way ANOVA analysis of indicated treatment pairs. **(c)** AngioSense retention signals in tumors on day 6 and *t*-test analysis. **(d)** The enhanced vascular leakiness further synergizes with RD-Sindbis/VEGF and promotes oncolytic replication of RC-Sindbis/Fluc vector in tumors. **(e)** Quantitative presentation of luciferase signals in tumors. **(f)** Relative growth curves and two-way ANOVA analysis.

Author Manuscript

Author Manuscript

Author Manuscript

Author Manuscript

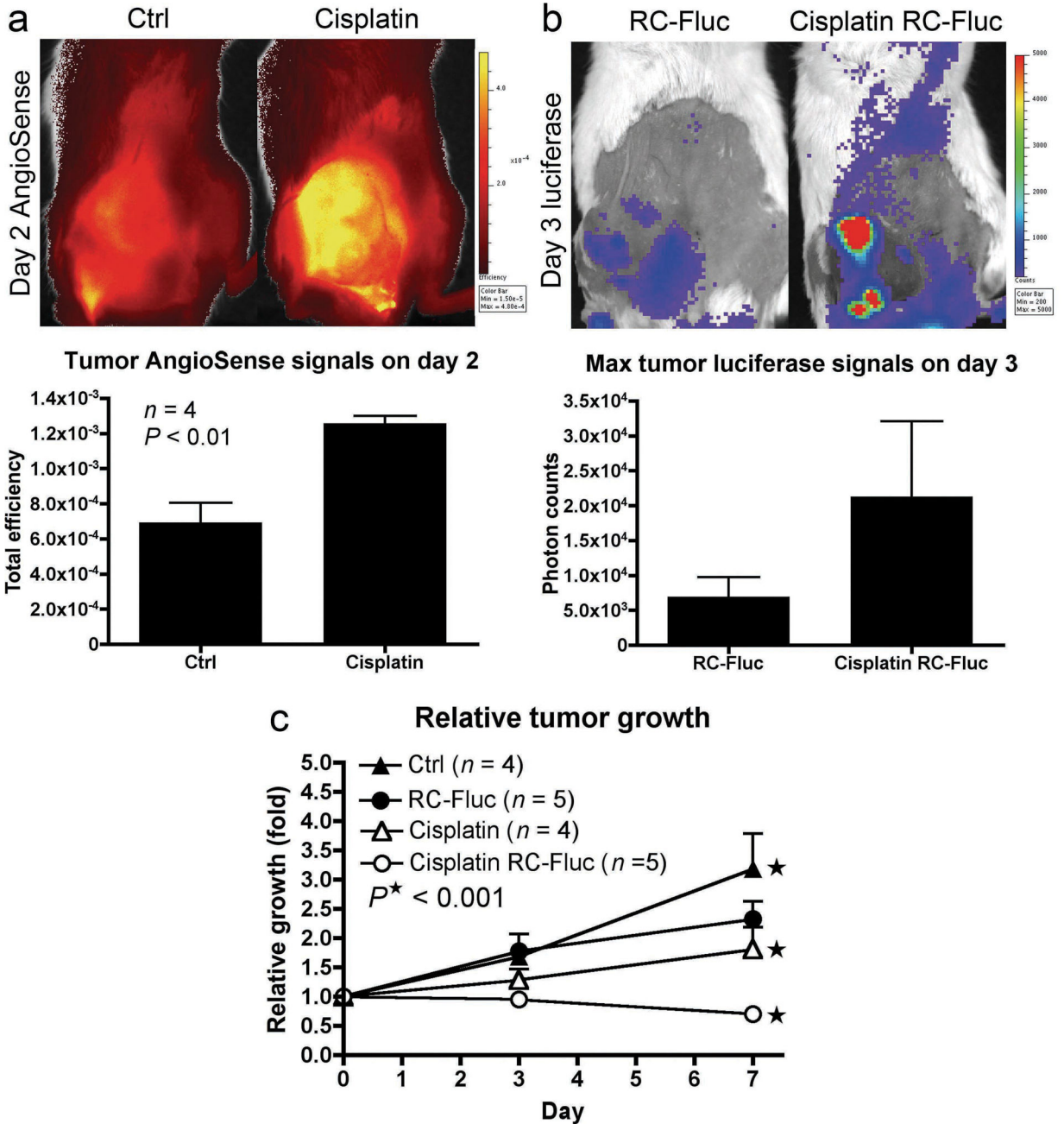


**Figure 6.** Cisplatin causes enhancement of tumor vascular leakiness and synergizes with oncolytic Sindbis vector in cancer therapy. Starting on day 0, daily treatments of cisplatin (4 mg/Kg or 12mg/m<sup>2</sup> compared with maximum tolerated dose of 100 mg/m<sup>2</sup> in human) were i.p. injected into SCID mice bearing s.c. N2a tumors. The last cisplatin treatment was administrated on day 4. **(a)** To visualize vascular leakiness, AngioSense 750 (0.66 nmol) was i.v. injected on day 1 and imaged on day 2. **(b)** RC-Sindbis/Fluc was i.v. injected on day 0 and day 2. Luciferase activities in tumors, indicating active vector propagation, were

monitored on day 3. (c) Relative tumor growth curves of different treatment groups. *P* value was generated by two-way ANOVA of trend.

Author Manuscript

Author Manuscript

Author Manuscript

Author Manuscript